On- and off-shell convergence of the time-independent mean-field theory of collisions

B. Giraud, M. A. Nagarajan,* and A. Weiguny†
Service de Physique Théorique, Centre d'Etudes Nucléaires de Saclay, 91191 Gif-sur-Yvette Cedex, France
(Received 20 February 1986)

The mean-field approximation to the many-body Green's function $(E-H)^{-1}$ is derived by the use of products of single particle orbitals for trial functions in a variational formalism. It is shown that the matrix elements of the Green's function behave smoothly as $\mathrm{Im}E$ is varied towards the on-shell limit $\mathrm{Im}E=0$.

I. INTRODUCTION

The evaluation of a many-particle Green's function $G=(E-H)^{-1}$, where H is the many-particle Hamiltonian composed of one- and two-body operators, is nontrivial when E is real and positive.[1] The evaluation of the collision amplitudes $\langle\chi'|T|\chi\rangle$ where χ and χ' are the initial and final channel vectors and $T=V'+V'GV$, where V and V' are the prior and post interactions, respectively, and G the total Green's function, requires a proper definition of G. In the case when many channels are open, where some of the channels may be three-or-more-fragment channels, the definition of G itself constitutes a complicated problem.

In a recent paper a time-independent mean-field theory of collisions was proposed.[2] This theory was based on three main ingredients, namely (i) a representation of the channels in terms of a basis of time-independent wave packets,[3] (ii) a variational principle which provided the representation of the matrix in terms of the stationary value of a functional,[4] and (iii) a restriction on the many body wave function to a space of products of single particle functions or Slater determinants.[5] The resulting mean-field equations satisfied by the single particle orbitals turned out to be generalizations of the usual Hartree (or Hartree-Fock) equations. The left-hand sides of these equations were determined by self-energies (η_i), one-body kinetic energy operators, and mean-field operators. The right-hand side of these equations were nonzero and described the source terms provided by the channels.

An alternate means of understanding these mean field equations is to seek the best product approximation $\overline{G}=\prod_i g_i$ to the exact many-particle Green's function, where $g_i=(\eta_i-h_i)^{-1}$ are single particle propagators. These are self-consistently deduced from the exact Hamiltonian H and channel vectors χ and χ'. The existence of the source terms in the generalized Hartree (or Hartree-Fock) equations illustrates how a many-body inversion, G, can be approximated by single-particle inversions, g_i. Several numerical applications[5-7] have proved this approximation to be extremely good.

In this paper we study the reasons why the product form $\overline{G}$ provides a good approximation to the exact G. We consider a matrix element of G between two square integrable functions χ and χ', where χ and χ' are themselves products of single particle functions. Such a simplification is merely for convenience, for the matrix element of G between the physical channel vectors can always be expanded in terms of the elements $\langle\chi'|G|\chi\rangle$: In Sec. II we state the variational principle and the mean-field equations. Two theorems are proved in Sec. III which prove, in turn, that the mean-field approximation becomes exact when $\mathrm{Im}E\to\infty$ for a fixed $\mathrm{Re}E$. The on-shell limit, $\mathrm{Im}E\to 0$, is investigated in Sec. IV in the case of an analytically soluble model and compared with a truncated subspace model. The summary and conclusions are provided in Sec. V.

II. VARIATIONAL PRINCIPLE AND MEAN-FIELD APPROXIMATION

It is first trivial to prove that the matrix element

$$D\equiv\langle\chi'|(E-H)^{-1}|\chi\rangle \tag{2.1}$$

is *the* stationary value of the functional of two trial functions ϕ,ϕ',

$$F\equiv\langle\phi'|\chi\rangle+\langle\chi'|\phi\rangle-\langle\phi'|(E-H)|\phi\rangle\ . \tag{2.2}$$

Indeed, the Euler-Lagrange equations for F read

$$0=\frac{\delta F}{\delta\phi}=\langle\chi'|-\langle\phi'|(E-H)\ , \tag{2.3a}$$

$$0=\frac{\delta F}{\delta\phi'^{*}}=|\chi\rangle-(E-H)|\phi\rangle\ , \tag{2.3b}$$

and hence

$$|\phi\rangle=G|\chi\rangle\ , \tag{2.4a}$$

$$\langle\phi'|=\langle\chi'|G\ . \tag{2.4b}$$

As long as $\mathrm{Im}E\neq 0$, G is a bounded operator and $E-H$ has G as its unique inverse. An insertion of Eqs. (2.4) into Eq. (2.2) just provides D, Eq. (2.1).

It is also trivial to consider the variational functional

$$F'=\frac{\langle\phi'|\chi\rangle\langle\chi'|\phi\rangle}{\langle\phi'|(E-H)|\phi\rangle}\ , \tag{2.5}$$

which also yields Eqs. (2.4), except for an arbitrary normalization for ϕ,ϕ'.

Even though χ,χ' are products of single particle orbitals, it is clear that ϕ,ϕ', Eqs. (2.4), are highly correlated states, for G is a complicated many-body operator. A simplification ansatz,

$$|\phi\rangle=\prod_i|\varphi_i\rangle\ , \tag{2.6a}$$

$$\langle \phi' | = \prod_i \langle \varphi_i' | \ , \tag{2.6b}$$

is thus a strong restriction. Conversely, F then has the simpler form (mean-field form)

$$\begin{aligned} \bar{F} = & \prod_i \langle \varphi_i' | \chi_i \rangle + \prod_i \langle \chi_i' | \varphi_i \rangle - E \prod_i \langle \varphi_i' | \varphi_i \rangle \\ & + \sum_i \langle \varphi_i' | t | \varphi_i \rangle \prod_{j \neq i} \langle \varphi_j' | \varphi_j \rangle \\ & + \sum_{i>j} \langle \varphi_i' \varphi_j' | v | \varphi_i \varphi_j \rangle \prod_{k \neq i,j} \langle \varphi_k' | \varphi_k \rangle \ , \end{aligned} \tag{2.7}$$

and there is trivially a similarly simple form $\bar{F}'$ for F'. Distinct particles have been considered in this Eq. (2.7), but antisymmetrization[5] would not be difficult to implement, obviously.

Elementary manipulations of $\bar{F}$ then provide the Euler-Lagrange equations

$$0 = \frac{\delta \bar{F}}{\delta \varphi_i'^*} = (\eta_i - h_i) | \varphi_i \rangle - \lambda_i | \chi_i \rangle \ . \tag{2.8a}$$

$$0 = \frac{\delta \bar{F}}{\delta \varphi_i} = \langle \varphi_i' | (\eta_i - h_i) - \lambda_i' \langle \chi_i' | \ . \tag{2.8b}$$

where λ_i, λ_i' are unessential normalization constants and one finds the (complex) self-energies

$$\begin{aligned} \eta_i = & E - \sum_{j \neq i} \frac{\langle \varphi_j' | t | \varphi_j \rangle}{\langle \varphi_j' | \varphi_j \rangle} \\ & - \sum_{\substack{k>j \\ j,k \neq i}} \frac{\langle \varphi_j' \varphi_k' | v | \varphi_j \varphi_k \rangle}{\langle \varphi_j' | \varphi_j \rangle \langle \varphi_k' | \varphi_k \rangle} \ . \end{aligned} \tag{2.9a}$$

and single particle Hamiltonians $h_i = t + U_i$ with

$$\langle r' | U_i | r \rangle = \sum_{j \neq i} \frac{\langle r' \varphi_j' | v | r \varphi_j \rangle}{\langle \varphi_j' | \varphi_j \rangle} \tag{2.9b}$$

in coordinate space, for instance. The Hartree nature of the mean field potential U_i acting upon orbitals φ_i, φ_i' is explicit from Eq. (2.9b). As discussed elsewhere,[5] exchange terms do not bring essentially new features to the theory.

The solutions of Eqs. (2.8) are then, for $\lambda_i, \lambda_i' = 1$,

$$| \varphi_i \rangle = g_i | \chi_i \rangle \ , \tag{2.10a}$$

$$\langle \varphi_i' | = \langle \chi_i' | g_i \ , \tag{2.10b}$$

to be compared with Eqs. (2.4). Here, $g_i = (\eta_i - h_i)^{-1}$, which means a linear inversion in single-particle space only, at the cost, however, of a nonlinear self-consistency because of the density dependences exhibited by Eqs. (2.9).

Once self-consistency for the orbitals φ_i, φ_i' is reached, an insertion of Eqs. (2.6) into the functional $\bar{F}'$, Eq. (2.5), provides an approximation $\bar{D}$ to D. It can be pointed out now, however, that our numerical studies[5-7] often yielded *several* different self-consistent solutions of Eqs. (2.9) and (2.10), while the original problem, Eqs. (2.4), has only one solution. This complication is due, obviously, to the nonlinear nature of the restrictive ansatz, Eqs. (2.6). Sections III and IV will take care of this multiplicity generated by the approximation.

III. THE LARGE WIDTH LIMIT

In this section we keep ReE fixed and consider the case where $\Gamma = \mathrm{Im}E \to +\infty$ (in the following we always retain $\Gamma \geq 0$, for the case $\Gamma \leq 0$ can be deduced trivially from the case $\Gamma \geq 0$). Since the norm of φ is arbitrary, we modify Eq. (2.4a) into

$$| \phi \rangle = \frac{E}{E - H} | \chi \rangle \ . \tag{3.1}$$

We then prove the following result.

Theorem 1: When $\mathrm{Im}E \to +\infty$, $| \phi \rangle$ has a strong limit equal to $| \chi \rangle$.

Proof: Define $\Delta\phi = \phi - \chi$. Then,

$$\langle \Delta\phi | \Delta\phi \rangle = \left\langle \chi \left| \frac{H^2}{(E^* - H)(E - H)} \right| \chi \right\rangle \ . \tag{3.2}$$

Expand $| \chi \rangle$ on the complete basis made by the eigenstates ψ_ϵ of H to obtain

$$\langle \Delta\phi | \Delta\phi \rangle = \int d\epsilon \rho(\epsilon) \frac{\epsilon^2}{(\mathrm{Re}E - \epsilon)^2 + \Gamma^2} \ , \tag{3.3}$$

where $\rho(\epsilon)$ is the spectral density of χ,

$$\rho(\epsilon) = | \langle \psi_\epsilon | \chi \rangle |^2 \ . \tag{3.4}$$

When $\Gamma \to +\infty$, the integrand in Eq. (3.3) converges simply towards zero for all values of ϵ and is uniformly bounded by the integrable function

$$M(\epsilon) = \left[\frac{(\mathrm{Re}E)^2}{\Gamma^2} + 1 \right] \rho(\epsilon) \leq 2\rho(\epsilon) \quad \text{if } \Gamma \geq \mathrm{Re}E \ . \tag{3.5}$$

Hence, by Lebesgue's theorem, $||\Delta\phi||$ vanishes when $\Gamma \to +\infty$.

Since we have chosen as a generic problem the case when χ is a factorized wave function, the limit of ϕ is thus factorized. An identical result holds for χ' as the limit of ϕ'. The mean-field theory becomes exact.

This conclusion is reinforced by the following result.

Theorem 2: The leading term of the amplitude D when $\Gamma \to +\infty$ is $\langle \chi' | \chi \rangle / E$.

Proof: One finds at once that

$$D - E^{-1} \langle \chi' | \chi \rangle = E^{-1} \langle \chi' | \Delta\phi \rangle \ , \tag{3.6}$$

and the right-hand side of Eq. (3.6) converges faster towards zero than Γ^{-1} since $||\Delta\phi|| \to 0$. A direct substitution of χ for ϕ and χ' for ϕ' in F', Eq. (2.5), yields the following correct leading term,

$$F' = \frac{\langle \chi' | \chi \rangle^2}{E \langle \chi' | \chi \rangle - \langle \chi' | H | \chi \rangle} \ , \tag{3.7}$$

provided, of course, that $\langle \chi' | H | \chi \rangle$ be finite.

In short, the limit behaviors of both D and ϕ, ϕ' are given by the mean field restriction. As a subsidiary result, we have checked numerically that, when $\Gamma \to +\infty$, there is at least one set of orbitals, solutions of the mean-field equations, Eq. (2.10) for which $\varphi_i \to \chi_i$, $\forall_i$.

It is now clear that a safe algorithm for the solution of Eqs. (2.10) consists of setting, at first, Γ large and using χ (χ') as a first guess for ϕ (ϕ'). Once self-consistency is reached, the obtained ϕ, ϕ' can be used as first guesses

with a slightly reduced value of Γ, and so on. The on-shell limit of the theory ($\Gamma=0$) will be reached this way as long as there is no bifurcation encountered along the path defined by the above algorithm.

The search for singularities on this path towards the real axis is the subject of the next section.

IV. THE ON-SHELL LIMIT

We already know from our numerical experiences[2-4] that the on-shell limit of the mean-field approximation seems to be a very smooth function of Γ and remains an excellent approximation for the exact amplitude. We have not been able to obtain a proof of this fact as general as the theorems of Sec. III. Instead, the following discussion is limited to the analytical model discussed in an earlier work.[7]

A. The model

This model first sets H real and $\chi=\chi'$ real, hence $\phi'=\phi^*$. Then $\mathscr{V}$ is set to vanish. This reduces Eqs. (2.8) to the simple form

$$(\eta_i-q^2)\phi_i(q)=\chi_i(q)\ , \tag{4.1}$$

in a momentum representation with q the single-particle momentum and $\hbar^2/2m=1$. A suitable symmetry group is imposed upon the orbitals χ_i in such a way that a complete degeneracy occurs between the orbitals. As a consequence, all the orbitals ϕ_i have the same kinetic energy,

$$\theta=\frac{\langle\varphi_i'\mid t\mid\varphi_i\rangle}{\langle\varphi_i'\mid\varphi_i\rangle}\ ; \tag{4.2}$$

hence the self-energies η_i are also degenerate,

$$\eta_i=E-(N-1)\theta\ . \tag{4.3}$$

The only self-consistent unknown is thus the self-energy η for Eqs. (4.1) solves according to

$$\varphi_i(q)=\frac{\chi_i(q)}{\eta-q^2}\ . \tag{4.4}$$

Here it is convenient to define the function

$$I(\eta)\equiv-\langle\chi_i\mid\varphi_i\rangle=\int\frac{\chi_i^2(q)}{q^2-\eta}\ ; \tag{4.5}$$

hence,

$$\theta=\int q^2\varphi_i^2(q)\left[\int\varphi_i^2(q)\right]^{-1}=\eta+I\frac{d\eta}{dI}\ , \tag{4.6}$$

and finally one obtains the unique self-consistency equation (SCE) to be solved in the model

$$\eta=E-(N-1)\eta-(N-1)I\frac{d\eta}{dI}\ . \tag{4.7}$$

The model becomes completely analytical if χ^2 is chosen as a Lorentzian,

$$\chi^2(q)=\frac{\gamma}{\pi}\frac{1}{(q-K)^2+\gamma^2}\ , \tag{4.8}$$

where γ is a width and K actually carries a subscript i which denotes the rotation of a fixed length vector under the symmetry group imposed upon the model. The choice of χ^2, Eq. (4.8), provides a contour integration for I, Eq. (4.5),

$$I(\omega^2)=-\frac{\omega+i\gamma}{\omega(\omega-K+i\gamma)(\omega+K+i\gamma)}\ ,\quad \mathrm{Im}\omega>0\ . \tag{4.9}$$

With $N=2$ as the simplest case, the SCE then becomes

$$\mathscr{P}(\omega)\equiv 2\omega^5+4i\gamma\omega^4+2(K^2-\gamma^2-E)\omega^3-5i\gamma E\omega^2$$
$$+4\gamma^2E\omega+i\gamma E(\gamma^2+K^2)=0\ . \tag{4.10}$$

Since K, as seen from Eq. (4.8), plays the role of a boost label for χ, the average kinetic energy carried by χ is of order K^2. It is thus convenient to set $E=2K^2+i\Gamma$ and consider cases where $K\gtrsim 2$ or 3 times γ, in order to separate this average momentum K from the zero-point fluctuations induced by γ. [It will be noticed, for what follows, that $\mathscr{P}(\omega)$ reduces to $\omega^3(\omega^2-K^2-i\Gamma)$ when $\gamma=0$.]

B. Absence of bifurcation

Among the five roots of the polynomial $\mathscr{P}$, Eq. (4.10), we find a "physical" one, ω_1, whose real part is of order K. Its imaginary part remains positive and small compared to K. Hence the corresponding self-energy $\eta^{(1)}=\omega_1^2$ has a real part of order K^2 and a positive imaginary part. When inserted into Eq. (4.4), this choice of η thus describes a retarded propagation of the single particle orbitals φ and corresponding trial function $\phi^{(1)}$. Conversely, there is another root ω_2 of $\mathscr{P}$ with the property $\omega_2\simeq-\omega_1^*$ when $\Gamma\simeq 0$. Hence the solution $\phi^{(2)}$ induced by $\eta^{(2)}=\omega_2^2\simeq\eta^{(1)*}$ may be interpreted as an advanced solution.

The solution $\phi^{(1)}$ is that solution which corresponds to theorem 1. Not only does it give an excellent approximation $\overline{D}$ to D when $\Gamma\to+\infty$ with $\mathrm{Re}E=2K^2$ fixed, but we also found in Ref. 3 that again $\overline{D}$ is very close to D when Γ is finite and also when $\Gamma\to 0$. This is a strong indication that the nonlinear problem, Eq. (4.10), has *no bifurcation* for the solution $\phi^{(1)}$ when Γ decreases from $+\infty$ towards 0.

This fact is illustrated by Fig. 1, which shows the trajectory of ω_1 when Γ decreases from 200 to 10 MeV and $\mathrm{Re}E=1000$ MeV (with $\hbar^2/2m=20$ MeV fm^2 for nuclear physics, this corresponds to Γ decreasing from 10 to 0.5 fm^{-2} and $\mathrm{Re}E=50$ fm^{-2}). The value taken for γ in this numerical application is $\gamma=0.5$ fm^{-1}, hence a scale of 5 MeV for single-particle energy fluctuations. We disregard in the following the fact that, in this Lorentzian model, $\langle\chi\mid\mathscr{T}\mid\chi\rangle$ is actually divergent, which contradicts a validity condition of Eq. (3.7).

Three main features stand out in Fig. 1. Firstly, the figure shows as solid lines a branch ω_1 and a branch ω_3 only. The branches ω_2 and ω_4 are absent because $\mathrm{Re}\omega_2$ and $\mathrm{Re}\omega_4$ are negative. The branch ω_5 for the fifth root of $\mathscr{P}$ is also absent because $\mathrm{Im}\omega_5$ is definitely negative, $\mathrm{Im}\omega_5\lesssim-\gamma$. Secondly, in the same way as $\omega_2\simeq-\omega_1^*$, the fourth root of $\mathscr{P}$ fulfills $\omega_4\simeq-\omega_3^*$, and these relations be-

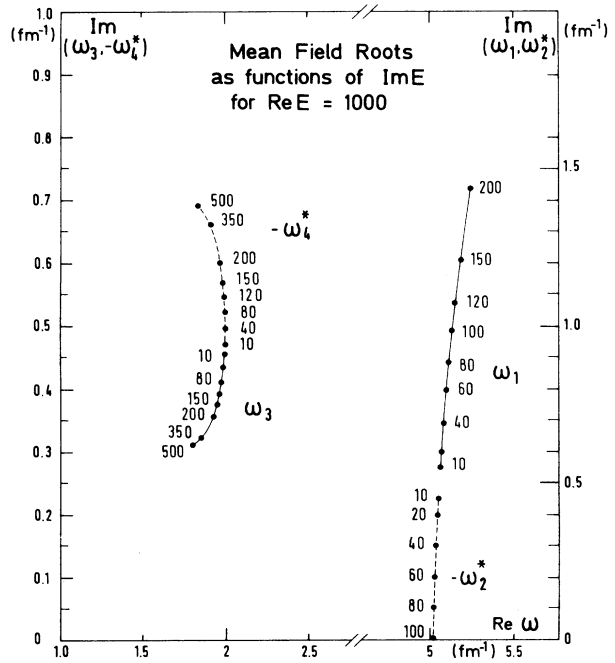

FIG. 1. Trajectories of two possible square roots ω_1,ω_3 of the mean field self-energy η when ImE decreases from 500 to 10 MeV. Associated trajectories for $-\omega_2^*$ and $-\omega_4^*$. The right-hand side scale is valid for ω_1 and $-\omega_2^*$, the left-hand scale for ω_3 and $-\omega_4^*$. The parameters are Re$E=1000$ MeV, $\gamma=0.5$ fm^{-1}, and $\hbar^2/2m=20$ MeV fm^2.

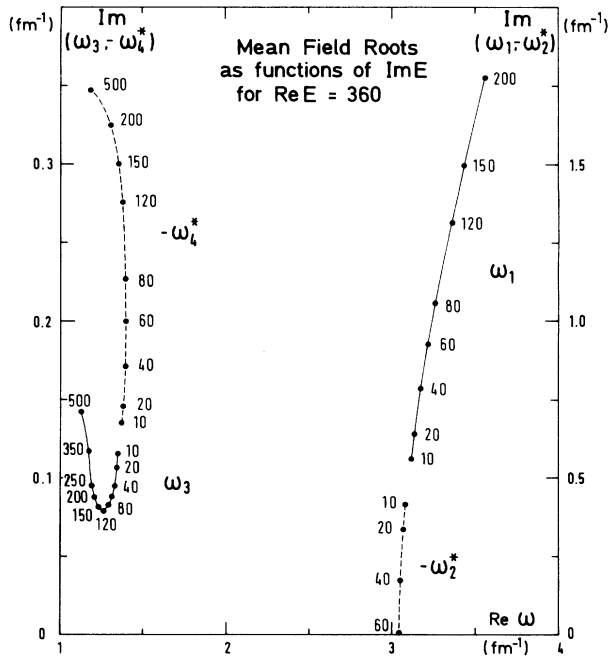

FIG. 2. Same as Fig. 1, except Re$E=360$ MeV.

come exact equalities when $\Gamma=0$. Hence Fig. 1 shows as dashed lines a branch $-\omega_2^*$ and a branch $-\omega_4^*$, which smoothly join the branches ω_1,ω_3, respectively. Thirdly, and this is the main conclusion to be drawn from this figure, these branches do not cross. There is *no bifurcation* in the domain investigated in this way.

The same conclusion and features stand out in Fig. 2, for which ReE is fixed at 360 MeV, corresponding to 18 fm^{-2}. More generally, in the domain we have explored ($100 \lesssim$ Re$E \lesssim 1000$ MeV), we have found no bifurcation of $\phi^{(1)}$ when Γ decreases from $+\infty$ to zero.

As a subsidiary result of some interest for the following, it is seen from Figs. 1 and 2 that, in the domain of parameters under consideration, there are at least three roots, ω_1, ω_3, and ω_4, which are acceptable under the condition Im$\omega>0$. The root ω_2 is also acceptable as long as Γ is small enough, for instance, $\Gamma \lesssim 100$ MeV, where Re$E=1000$ MeV. Even though the physical solution is now recognized to be $\phi^{(1)}$, the other solutions $\phi^{(3)}$, $\phi^{(4)}$, and whenever acceptable, $\phi^{(2)}$, do span a subspace of wave functions which deserve consideration for a linear expansion of an improved trial function in the variational principle, Eq. (2.2). This linear projection of the variational principle in a truncated subspace is the subject of the following subsection.

C. Comparison with a truncated linear approximation

As stated already, the mean-field method is a nonlinear approximation to the linear, but untractable, problem described by Eqs. (2.4). A restriction of this linear problem to a finite dimensional subspace of the Hilbert space, however, obviously becomes tractable. It is trivial, then, that the truncated Hamiltonian (projected in that subspace) has a discrete spectrum only. Whenever the imaginary part Γ of the energy is larger than, or of the same order of magnitude as, the average splitting ΔE between the discrete eigenvalues of the projected Hamiltonian, some matrix elements $\bar{\bar{D}}$ of the propagator $(E-PHP)^{-1}$ may be reasonable approximations of the corresponding matrix elements D of the exact propagator G. Conversely, we expect $\bar{\bar{D}}$ to be definitely unreliable if $\Gamma \ll \Delta E$.

The spectrum $\{E_n\}$ of PHP is shown in Figs. 3 and 4 as a function of Γ for Re$E=1000$ and 360 MeV, respectively. The subspace defined by the projector P not only includes $\phi^{(1)}$, $\phi^{(3)}$, $\phi^{(4)}$, and whenever acceptable, $\phi^{(2)}$, but also their complex conjugates. In short, there are states $\phi^{(5)}=\phi^{(1)*},\ldots,\phi^{(8)}=\phi^{(4)*}$. This inclusion of complex conjugates is designed to preserve time reversal invariance of the subspace, an important precaution in a theory of collisions. This is why Fig. 3 shows, e.g., eight eigenvalues when $\Gamma<100$ MeV and six eigenvalues when $\Gamma>100$ MeV. An inspection of Fig. 3 shows that in the energy range $E_n \simeq 1000$ MeV the level splitting is $\Delta E \simeq 50$ MeV. Very similar properties are shown by Fig. 4 with

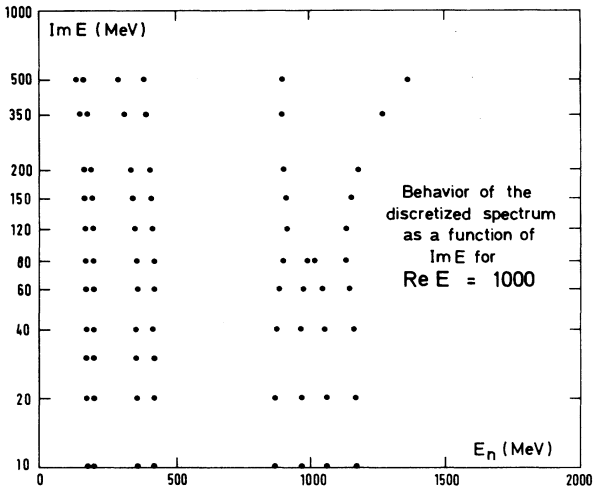

FIG. 3. Spectrum of the projected Hamiltonian in the subspace spanned by $\phi^{(1)},\ldots,\phi^{(4)*}$. When $\mathrm{Im}E>100$ MeV the subspace has dimension 6 only.

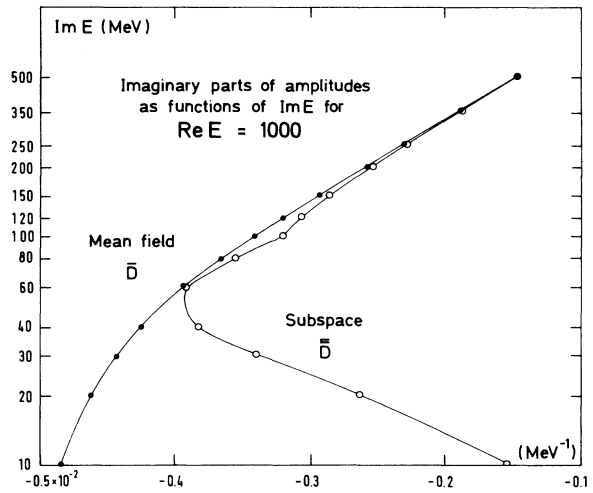

FIG. 5. Comparison of the mean-field amplitude $\overline{D}$ with the amplitude $\overline{\overline{D}}$ provided by linear truncation. Notice the abrupt deviation of the latter when $\mathrm{Im}E$ becomes smaller than the level splitting in the truncated spectrum ($\Delta E\simeq 50$ MeV).

$\mathrm{Re}E=360$ MeV. It thus makes sense to compare the mean-field amplitude $\overline{D}$ with the truncated amplitude

$$\overline{\overline{D}}=\langle\chi\,|\,P(E-PHP)^{-1}\,|\,\chi\rangle\ , \tag{4.11}$$

as long as $\Gamma\gtrsim 50$ MeV. The latter amplitude, $\overline{\overline{D}}$, can be calculated, obviously, by a numerical inversion of the six- or eight-dimensional matrix $EP-PHP$.

The results are shown in Figs. 5 and 6 for the comparison of the imaginary parts of $\overline{D}$ and $\overline{\overline{D}}$ against each other and with, again, $\mathrm{Re}E=1000$ and 360 MeV, respectively. As soon as $\overline{\overline{D}}$ ceases to be reliable (at low values of Γ), it deviates from $\overline{D}$. For higher values of Γ, $\overline{\overline{D}}$ and $\overline{D}$ are essentially equal (whether one considers their real or their imaginary parts).

Agreement of $\overline{D}$ and $\overline{\overline{D}}$ when $\Gamma\gtrsim\Delta E$ and contradiction of $\overline{D}$ and $\overline{\overline{D}}$ when $\Gamma\lesssim\Delta E$, added to the knowledge that $\overline{\overline{D}}$ is wrong when $\Gamma\lesssim\Delta E$, does not comprise sufficient evidence that $\overline{D}$ is reliable when $\Gamma\lesssim\Delta E$. The smooth behavior of $\overline{D}$, however, for all values of Γ, does give an increased confidence in the reliability of the on-shell limit of $\overline{D}$. Last but not least, a numerical calculation of the exact D by brute force integration of $(E-\mathscr{T})^{-1}$ in a momentum representation does show that $\overline{D}$ and D remain very close to each other when $\Gamma\to 0$.

The conclusion to be drawn from this analysis is that the nonlinear approximation $\overline{D}$ is usually better than, or at least as good as, the truncated linear approximation $\overline{\overline{D}}$. As a matter of curiosity we show in Table I the components of the truncated trial state

$$|\,\overline{\overline{\phi}}\rangle=\frac{P}{E-PHP}\,|\,\chi\rangle\ , \tag{4.12}$$

when expanded in the basis $\phi^{(1)},\ldots,\phi^{(4)*}$. For large values of Γ, $\overline{\overline{\phi}}$ is just dominated by $\phi^{(1)}$, as expected. For

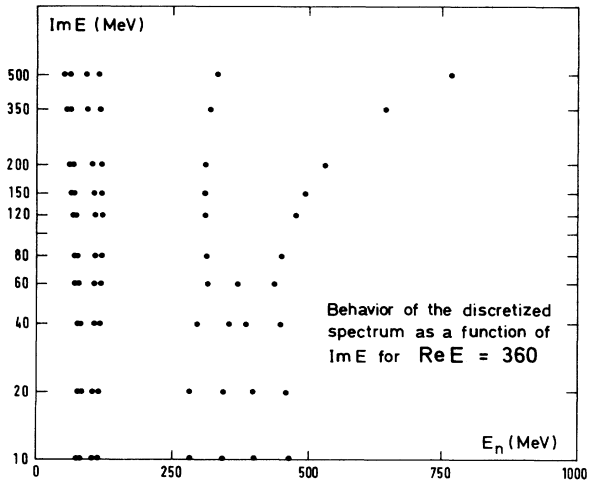

FIG. 4. Same as Fig. 1 for $\mathrm{Re}E=360$ MeV.

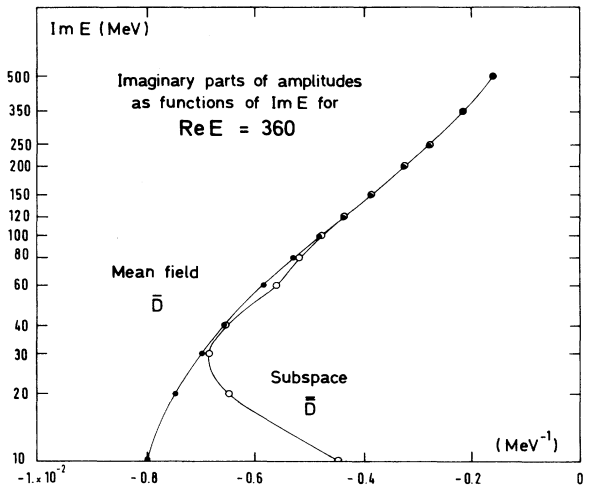

FIG. 6. Same as Fig. 5 for $\mathrm{Re}E=360$ MeV.

TABLE I. Dominant components of the truncated linear trial state $\bar{\bar{\phi}}$. The top half of the table corresponds to Re$E=1000$ MeV and the bottom half to Re$E=360$ MeV. The states $\phi^{(2)}$ and $\phi^{(2)*}$ are not accepted in the subspace when Im$E>100$ MeV in the former case and Im$E>60$ MeV in the latter. Effects of deviation of $\bar{\bar{D}}$, because of the level density, occur when Im$E<60$ and 40 MeV, respectively. Only the main components are shown, in arbitrary units.

ImE (MeV)	1	2*	3	4*	1*	2	3*	4
				Re$E=1000$ MeV				
150	$5i$	· · ·				· · ·		
120	$6i$	· · ·		i	$-i$	· · ·		
100	$6i$		$-i$	i	$-i$			
80	$6i$	$2i$	$-i$	i	$-i$			
60	$4i$	$1+5i$						
40	$-1-2i$	$2+11i$	$3i$	$-4i$	$2+5i$	$-2-5i$	$-2-3i$	$3+3i$
				Re$E=360$ MeV				
120	$1+6i$	· · ·				· · ·		
100	$1+7i$	· · ·				· · ·		
80	$2+8i$	· · ·			$-i$	· · ·		
60	$2+10i$				$-1-2i$			
40	$8i$	$3+6i$						
30	$-3+3i$	$5+12i$			$2+3i$	$-3-3i$		

low values of Γ, $\bar{\bar{\phi}}$ becomes much more collective, but it is still dominated by $\phi^{(1)}$ and/or $\phi^{(2)*}$. As seen in Figs. 1 and 2, $\eta^{(1)}$ and $\eta^{(2)*}$ are very similar when Γ is small, anyhow, and hence a dominance of $\phi^{(1)}$ is still present. The other components on $\phi^{(2)},\phi^{(3)},\ldots$ are not negligible when Γ is small, however. It will be noticed again that $\phi^{(3)}$ and $\phi^{(4)*}$ are then quite similar, and the same holds for $\phi^{(1)*}$ and $\phi^{(2)}$. Hence the opposite components shown by Table I induce a large amount of compensation. Even though $\bar{\bar{\phi}}$ is not really reliable, this configuration mixing at low Γ is likely to show subtle and intriguing properties.

To summarize this long section, we have identified a well defined mean-field solution $\bar{\phi}=\phi^{(1)}$ which does not bifurcate when $\Gamma\to 0$ and which provides a much smoother (and more accurate) on-shell limit than the most natural linear approximations, $\bar{\bar{\phi}}$, available. This is strong evidence that the mean-field amplitude $\bar{D}$ is a reliable approximation, whether Γ is large or small.

V. DISCUSSION AND CONCLUSION

The mean-field approximation of the Green's function appears to be a precise and practical tool for the theory of collisions. As it is nonlinear and generates, at first, several possible answers for a unique (linear) problem, it raises a difficult problem of spuriosity elimination. We have definitely identified the unique, physical solution, which is well behaved both when ImE is large and ImE is small. Subsidiary conditions such as Re$E\gg\gamma^2$ or Im$E\gtrsim\gamma^2$, which take into account energy fluctuations in wave packets, may be necessary to ensure better validity of our method in practical cases, but there is no doubt that the mean-field method has a smooth on-shell limit, because the single-particle energies $\eta^{(1)}$ remain complex while E becomes real.

This remarkably smooth on-shell limit is best illustrated by Figs. 7 and 8, which are contour plots of the modulus of the mean-field functional $\bar{F}'$ as a function of $\omega=\sqrt{\eta}$. As seen from Eqs. (4.9) and (4.6), an analytic continuation of our functional

$$\bar{F}'=\left[I^2\frac{d\eta}{dI}\right]^N\left[E-N\eta-NI\frac{d\eta}{dI}\right]^{-1}$$

is trivial away from the critical values $\omega_1,\ldots,\omega_5$ of the trial function parameter ω. The flat[8] nature of the physical saddle point ω_1 is illustrated in Fig. 7, which maps out $|\bar{F}'|$ for Re$E=360$ MeV, strictly on-shell ($\Gamma=0$). For the sake of completeness, we show in Fig. 8 the more con-

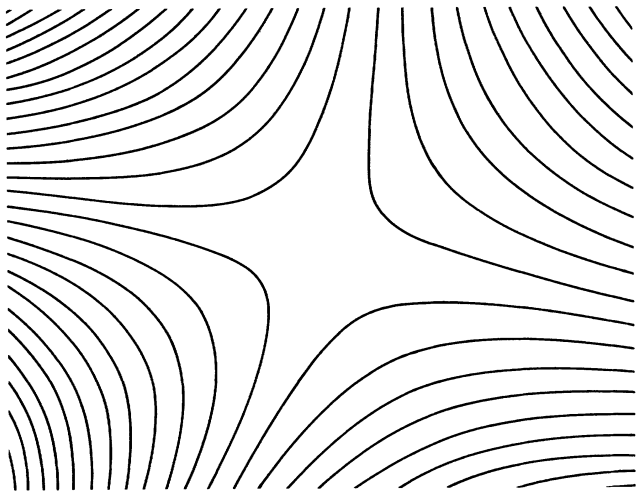

FIG. 7. Contour plot of the variational functional $|\bar{F}'|$ around the physical saddle point $\omega_1=3.10+0.49i$ fm^{-1} for $E=360$ MeV. From the low equipotentials to the high equipotentials the functional varies by less than 10%. From top to bottom Imω runs from 0.7 to 0.3 fm^{-1} and from left to right Reω runs from 2.9 to 3.3 fm^{-1}.

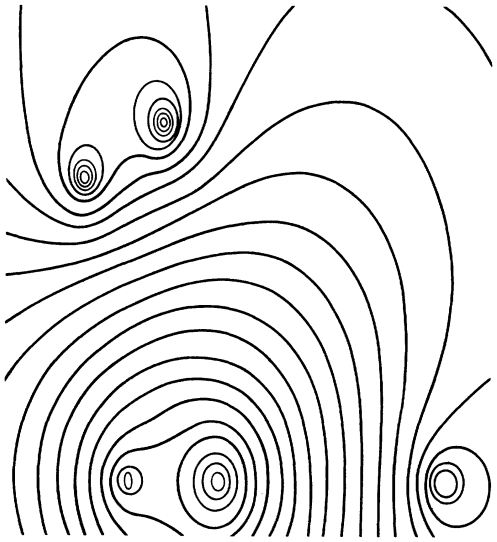

FIG. 8. Contour plot of $|F'|$ for $E=360+60i$ MeV. From top to bottom Reω runs from 1.8 to -0.2 fm^{-1} and from left to right Imω runs from 0.7 to -2.3 fm^{-1}. The saddle point at the top left is $\omega_3=1.31+0.09i$ fm^{-1}. That at the bottom right is $\omega_5=-(0.09+2.22i)$ fm^{-1}. An additional saddle point at $\omega=0$ is found as an artifact because we use the "ω" complex plane rather than the "ω^2" complex plane. The functional varies by 10 orders of magnitude in this domain.

trasted behavior of $|\bar{F}'|$ in the neighborhood of "spurious" saddle points ω_3 (top left) and ω_5 (bottom right). Sharp peaks of $|\bar{F}'|$ in the vicinity of ω_3,ω_5 denote poles, and likely "resonances" or "bound states" associated with them, while the vicinity of ω_1 shows no such singularity. We have a whole atlas of such plots with various values of ReE and Γ (actually, Fig. 8 corresponds to $\Gamma=60$ MeV) with the same general conclusion; namely the contour plots of $\bar{F}'$ evolve smoothly into one another as ReE and Γ span the physical region of interest, and the saddle points ω_1 and ω_2 are flatter than the saddle points ω_3, ω_4, and ω_5.

In particular, the on-shell plots show no special property, except for the exact symmetry relating ω_1 to ω_2, for instance, as discussed in Sec. IV B and Ref. 3. It can be concluded that not only the mean-field amplitude $\bar{D}$, calculated as the stationary value $\bar{F}'(\omega_1(\Gamma),\Gamma)$ at the saddle point ω_1, has a smooth limit, but also that the doubly analytic function $\bar{F}'(\omega,\Gamma)$ of two independent variables ω and Γ has only isolated singularities when $\Gamma\to 0$.

In a future paper we intend to verify the validity of the on-shell limit of our mean-field method for more general models, including interactions. It may be stressed already here that the validity of theorems 1 and 2 (the large Γ limit) is already established for nonsingular potentials. This general result is readily seen from the argument of Sec. III.

ACKNOWLEDGMENTS

It is a pleasure to thank R. Balian for his interest in this problem and for stimulating discussions. A pleasant interaction with Y. Abe, Y. Hahn, and S. Kessal is also gratefully acknowledged. The help of C. Verneyre for the numerical applications is gratefully appreciated. This work has benefited from partial support by NATO Grant No. 606/84.

---

*Permanent address: Daresbury Laboratory, Daresbury, Warrington WA4 4AD, United Kingdom.

†Permanent address: Institut für Theoretische Physik, Universität Münster, Domagkstrasse 71, Münster, Federal Republic of Germany.

[1]D. J. Kouri and F. S. Levin, J. Math. Phys. **14**, 1637 (1968); Nucl. Phys. **A253**, 398 (1975); W. Tobocman, Phys. Rev. C **9**, 2466 (1974); **12**, 741 (1975).

[2]B. G. Giraud, M. A. Nagarajan, and I. J. Thompson, Ann. Phys. (N.Y.) **152**, 475 (1984).

[3]B. G. Giraud and M. A. Nagarajan, J. Phys. (Paris) **41**, 477 (1980).

[4]B. G. Giraud and M. A. Nagarajan, J. Phys. G **4**, 1739 (1978).

[5]B. G. Giraud, M. A. Nagarajan, and C. J. Noble, Phys. Rev. A **34**, 1034 (1986).

[6]Y. Abe and B. G. Giraud, Nucl. Phys. **A440**, 311 (1985).

[7]B. G. Giraud, Physica **19D**, 112 (1986).

[8]We thank R. Balian for a stimulating comment on this fact.